Talanta 120 (2014) 141–147

Contents lists available at ScienceDirect

Talanta

journal homepage: www.elsevier.com/locate/talanta

DNA nanomachines as evolved molecular Beacons for in vitro and in vivo detection

Shuo Feng [a,1], Ye Shang [b,1], Fan Wu [a], Fei Ding [a], Bin Li [a], Jiahui Xu [a], Liang Xu [a,*], Xiang Zhou [a,c,**]

[a] College of Chemistry and Molecular Sciences, Key Laboratory of Biomedical Polymers of Ministry of Education, State Key Laboratory of Virology, Wuhan University, Wuhan, Hubei, 430072, PR China
[b] College of Life Sciences, Wuhan University, Wuhan, Hubei, 430072, PR China
[c] State Key Laboratory of Natural and Biomimetic Drugs, Peking University, Beijing, PR China

ARTICLE INFO

Article history:
Received 26 September 2013
Received in revised form
12 November 2013
Accepted 13 November 2013
Available online 13 December 2013

Keywords:
Nanomachine
Molecular beacon
Nucleic acids
Cell imaging
Biosensors

ABSTRACT

Modern biosensors require high sensitivity, great signal enhancement and extensive applicability for detection and diagnostic purposes. Traditional molecular beacons (MBs) do not meet these requirements because of the lack of signal amplification. The current amplification pathways using enzymes, DNAzymes and nanoparticles are usually quite sophisticated and are limited to specific applications. Herein, we developed simple biosensors based on the structure of kissing-hairpin. Through hybridization amplification of these nanomachines, the evolved MBs could greatly enhance the detected signals (approximately 10-fold higher than the signals generated by traditional molecular beacons), reduce the sensing limits for targets and, remarkably, distinguish single-base mismatches specifically for nucleic acid detection. In addition, these new MBs can be directly applied in living cells. By introducing aptamer sequences, these novel sensors can also detect proteins and small molecules. These properties were exemplified by the detection of both the β-actin gene and thrombin. The simplicity, sensitivity and flexibility of these devices make them appropriate for more expansive applications.

1. Introduction

Molecular beacons (MBs), which are designed DNA hairpin structures that were first introduced in 1996 [1], have been widely applied in nucleic acid detection, biosensor development, gene monitoring in living systems and protein investigations [2,3]. Despite their good sensitivity and specificity for biomedical targets, the primary advantages of MBs are their structural simplicity and flexibility. For example, MBs can be placed on the surfaces of nanoparticles [4–6] and electrodes [7,8] or linked to solid carriers for the fabrication of biochips [9,10]. However, classic MBs cannot meet the requirements of high sensitivity, signal enhancement and selectivity for detection and diagnostic purposes. There have been numerous attempts over the past decade to optimize and modify the hairpin structures [11] and, most importantly, to develop complex signal amplification systems. Various optically and electrically amplified biosensors have been developed using enzymes [12–17], DNAzymes [18–21] and nanoparticles [4–6,22] as amplification labels. One common enzymatic amplification method used for ultrasensitive DNA detection is rolling circle amplification, an isothermal process mediated by certain DNA polymerases to generate long single-stranded (ss) DNA molecules from a short circular ssDNA template [23]. Some enzymes, such as ligase [15], exonuclease III [16], and nicking enzymes [17], have also been reported to efficiently amplify signals for the detection of nucleic acids, proteins and small biomolecules. DNAzyme-based amplifications and combinations of protein enzymes and DNAzymes [12,15,24] have both been used as sensing platforms. Although enzyme-based catalytic pathways are efficient and result in low detection limits, their complexity and inflexibility make these methods inconvenient for extensive applications. Another issue is that the detection behavior is strongly dependent on the catalytic activity of the enzyme.

Another amplification pathway is based on the use of nucleic acid hybridization as an energy source to drive changes in configuration [25,26]. For example, strand displacement could be used to catalyze the release of a specified output oligonucleotide to amplify nucleic acid signals [27–29]. DNA hairpin structures, which are ideal components of DNA nanomachines and assemblies [25,26,30] because of their unmatched loops, could be used in the

* Corresponding author.
** Corresponding author at: College of Chemistry and Molecular Sciences, Key Laboratory of Biomedical Polymers of Ministry of Education, State Key Laboratory of Virology, Wuhan University, Wuhan, Hubei, 430072, PR China.
Fax: +86 27 87336380.
E-mail address: xzhou@whu.edu.cn (X. Zhou).
[1] S. Feng and Y. Shang contributed equally to this work.

0039-9140/$ - see front matter © 2013 Elsevier B.V. All rights reserved.
http://dx.doi.org/10.1016/j.talanta.2013.11.038

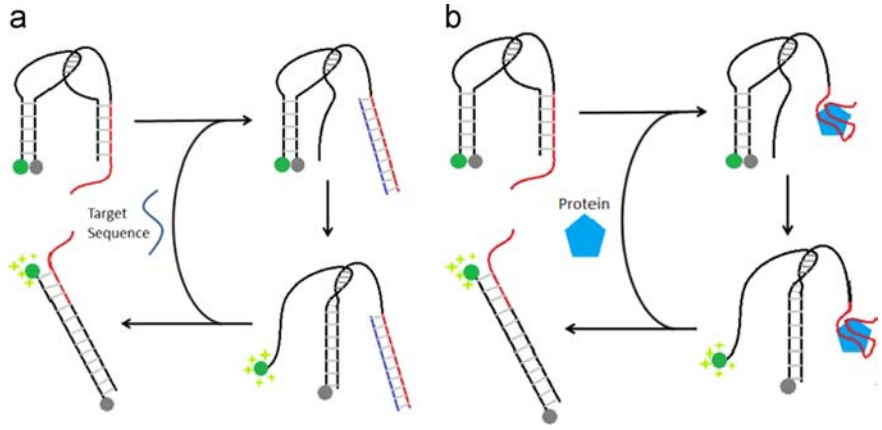

Scheme 1. Biosensors based on autonomous DNA devices. Nucleic acids (a) or proteins (b) open hairpins through external toehold to activate autonomous hybridization, along with fluorescence respond. Targets are then displaced from hairpins again to trigger another hybridization process.

hybridization chain reaction (HCR) to achieve signal amplification [31], and have been used to enable the imaging of mRNA expression [32]. Unlike enzymatic amplification, amplification powered by hybridization only involves nucleic acids, and thus it is not influenced by as many environmental factors and can operate under conditions that might otherwise inhibit enzymes. To further the goal of signal amplification, Turberfield et. al. introduced MB hairpin structures into an autonomous DNA device powered by hybridization [33], as shown in Scheme 1. The classic MB interacts with another complementary hairpin structure to form a dimeric complex called a "kissed" structure, as previously observed [33,34]. In addition to forming a kissed structure, the two hairpins can also form a duplex in a slow but spontaneous and detectable process [33–36], inhibiting the direct use of these two hairpins for amplification. This kissed complex is almost impossible to transform into the more stable duplex unless a "catalyst" is present (see Scheme 1 for an illustration). This catalyst can be either a target nucleic sequence that opens one of the hairpins or a protein or small molecule that interacts with the aptamer sequence in the hairpin, as described in Scheme 1. The catalyst first interacts with the specifically recognized hairpin structure to open the stem, making the other nucleotides within the stem available for hybridization with the complementary hairpin. This process displaces the catalyst from the hairpin again, thus making it available for another catalysis cycle. After the addition of the catalyst, the kissing hairpins can autonomously form duplexes, resulting in fluorescence enhancements. Because the catalyst is recycled, the fluorescence signals can be effectively amplified.

In this study, we took advantage of the structure of kissing-hairpin and developed our own detection nanomachine- amplified MBs (AMBs). Compared with traditional MB (TMB), AMB revealed its pronounced capability in sensitivity, selectivity and wide range of applications. Obvious advantages of AMBs in detecting target DNA was observed by kinetic monitoring of the TMB and its corresponding AMB. AMB could also remarkably distinguish the perfect match from single-base mismatches specifically for nucleic acid detection. Moreover, AMB was not only aim at DNA detection, but widely applied in protein detection by changing the binding region to aptamer sequence. Since AMB was operated by only hybridization, it was not influenced by environmental factors and can perform in living cell condition. Therefore, this nanomachine could trigger signal amplification for in vivo detection. Compared with traditional TMBs, AMB can greatly enhance signal detection and decrease the sensing limits for targets.

2. Materials and methods

2.1. Materials

DNA sequences used in this work are listed in Table S1. All the fluorescence labeled oligonucleotides were purchased from TaKaRa Clontech. All the unlabeled sequences were purchased from Invitrogen Company. Thrombin was purchased from Sigma. All the experiments were performed in the TAE/Mg^{2+} buffer (10 mM Tris-Acetic acid, 1 mM EDTA and 10 mM Mg^{2+}; pH=8.0).

2.2. Formation and purification of kissing hairpins

The hybridization was performed in TAE/Mg^{2+} buffer. Before use, hairpins were formed by heating to 95 °C at 20 μM concentration in this buffer, then cooling to 4 °C rapidly, and subsequently maintaining at room temperature for over 2 h. Quenching avoids the formation of homodimers and larger complexes by hybridization of neck domains from different oligonucleotides. Then the traditional MBs could be obtained. To form kissing hairpins, the two corresponding hairpins were mixed together with equal amount, followed by keeping the mixtures at room temperature for over 2 h to achieve totally kissing. Then the kissing hairpins were purified through native gel electrophoresis. The gel electrophoresis was run on 16% polyacrylamide gel at 4 °C, 12 V/cm in TAE/Mg^{2+} buffer. The kissing bands were cut from gels, and then eluted with TAE/Mg^{2+} buffer at 20 °C. The purified solutions of kissing hairpins were quantified by UV absorbance at 260 nm.

2.3. Fluorescence kinetic experiments

Fluorescence data were recorded using Perkin-Elmer LS55 Fluorescence Spectrometer with the temperature controller set to 25 °C. Excitation and emission wavelengths were 515 and 535 nm, respectively, with 10 nm bandwidths. The fluorescence data of 50 or 25 nM kissing complexes in 400 μL solutions were collected for 5 or 10 min before addition of targets. The runs were paused for about 1 min to add 4 μL of targets at the required concentrations and mix by gentle pipetting. All the experiments contained three parallel groups, and showed good stability and reproducibility.

2.4. Detection of miR-141 using AMBs

A 100 μL reaction mixture containing DEPC treated water, 40 U RNase inhibitor, 50 nM AMB and the target miR-141, the reaction system was incubated at 37 °C for 2 h. Following the incubation, the reaction mixture was transferred to a 96-well plate to measure fluorescence signal. The excitation wavelength was 488, and the emission wavelength was 530 nm. Fluorescence emission spectra were scanned with the Pharos FX Molecular imager. We repeated the detection for three times, all demonstrated great enhancement and good stability.

2.5. Cell culture

HeLa cells (CCTCC, China) were cultured in MEM (Hyclone, China) supplemented with 10% FBS (Hyclone) and penicillin (100 units/ml). MDA-MB-231(CCTCC, China) cells were cultured in DMEM (Hyclone, China) supplemented with 10% FBS (Hyclone) and penicillin (100 units/ml). All the cells were incubated at 37 °C in a 95% humidified atmosphere containing 5% CO_2.

2.6. Transfection

The probes (100 pmol) were transfected into living cells by using Lipofectamine 2000 (Invitrogen) in 35-mm glass-bottomed dishes (Nest). After incubated at room temperature for 4 h, the transfection mixture was removed and fresh medium was added. Then the cells would be incubated at 37 °C for 4 h.

2.7. Fluorescence microscopy

After the cells were prepared, they would be washed with PBS three times, then mounted on the microscope stage. Confocal images were taken using Carl Zeiss LSM 710. The excitation wavelength was 488, and the emission wavelength was 530 nm (green fluorescence). Four parallel samples were detected, stability and reproducibility of the AMB detection system could be observed.

3. Results and discussion

Here we first investigated the DNA detection ability of an AMB using an asymmetric kissed complex composed of two fully complementary sequences, whose structure has been reported previously [33,34], to illustrate the advantages of this strategy. This AMB could be considered a TMB matched with its complementary amplifying-assistant hairpin. The hairpin was opened through an internal toehold, as shown in Fig. S2 in the Supporting Information. We selected this asymmetric AMB as a model to allow direct comparison with the TMB to reveal the advantages of the AMB. The formation and purification of this AMB are described in the Supporting Information. The AMB was used in the same manner as TMBs, an advantage over other sophisticated amplification procedures. After the addition of the catalytic DNA, also called the target DNA, the AMB can be opened to generate the fluorescent signals. Parallel experiments were also performed with the corresponding TMB (indicated in Fig. S2) that contained the same hairpin but not its complementary hairpin. The AMB and TMB were compared based on the detection limit, the level of signal enhancement and the ability to detect a single-base mismatch.

All detection experiments for both the AMB and TMB methods were performed using the same procedure in the same environment. The TMB was able to detect 1 nM target DNA, similar to other reported MBs [2], but failed to sense DNA at a concentration of 100 pM, as shown in Fig. 1a. The AMB tested here effectively recognized 100 pM target DNA with an even stronger signal than that for the TMB at 1 nM target (Fig. 1a). The AMB was able to greatly amplify the signal through catalytic hybridization, leading to more sensitive detection. In addition to lower detection limits, remarkable signal enhancement was also observed, as shown in Figs. 1a and S2. For example, when detecting 1 nM DNA, target DNA bound to the recognized hairpin structure, opened the stem and started the next cycle. Then the kissing structures autonomously formed duplexes resulting in fluorescence enhancements. Otherwise, one TMB could merely detected one target DNA correspondingly. The AMB signal was 10-fold higher than the TMB signal. These two advantages of the TMB are both relevant to their application as biosensors. In addition to the low detection limit, which was the original goal, the ability to recognize targets with strong signal enhancement enables the target signal to be distinguished from the signals of interfering factors.

The AMB developed in this study based on catalytic autonomous motion not only provided an amplification pathway but also strengthened the ability to detect single-base mismatches. Using the above AMB as an example, we evaluated the ability of AMBs to detect single-base mutations. A sequence with a single-base mutation from A to T was selected to test both the TMB and the AMB (Table S1). Faced with this single-base mutation, the TMB distinguished the target DNA from the mutated sequence poorly, with less than a 2-fold difference in the signal strength. However, the AMB was able to efficiently recognize the target DNA, with an almost 20-fold greater signal response relative to that of the mutated DNA (Fig. 1b). The strong ability of AMB to distinguish the target sequence and a single-base mismatch sequence is an interesting phenomenon. The recognition of target DNA in the presence of mutated sequences is usually based on their different thermodynamic properties. For TMBs, target DNA can completely open the rationally designed hairpin structure, whereas the mutated sequences cannot open the MB completely because of the relatively low thermo stability of the opened MB. The kinetic rate of hairpin opening by the mutated sequence was also much lower than that of opening by the target DNA. The rate constant for opening this TMB with the target DNA was $2.54 \times 10^7\ M^{-1}\ min^{-1}$, whereas this value was $5.80 \times 10^6\ M^{-1}\ min^{-1}$ with the single-base mutated sequence, 2-fold lower than that for the target DNA (see the ESI for the kinetic calculations). This AMB, evolved from the TMB, obviously still possessed the same thermodynamic properties but exhibited different kinetic characteristics. The kinetic distinction between the target and mutated DNAs was greater for the AMB, with a 14-fold difference ($7.25 \times 10^5\ M^{-1}\ min^{-1}$ for the target sequence vs. $6.13 \times 10^4\ M^{-1}\ min^{-1}$ for the mutated sequence, Fig. S2), greatly improving the ability to recognize the desired sequence.

After confirming the superiority of the AMB, we next used this autonomous DNA machine for gene and protein detection. For real detection applications, however, the fully asymmetric AMBs, such as the one above, have a significant disadvantage in that the detection process takes several hours because the amplification, which is activated by an internal toehold, is too slow to enable a rapid response. Thus, we introduced external toeholds into the hairpin structures, which have been previously reported to accelerate the opening rate [33,37]. In this case, the labeled fluorescence and quenching groups must be moved from the detecting hairpins to the amplifying-assistant hairpins. Using this asymmetrical kissed structure, we attempted to detect the DNA sequence for the β-actin gene and a protein, thrombin (see Scheme 1).

The selected gene sequence for β-actin was able to open its target hairpin through an 8 nt external toehold to facilitate hybridization (Table S1). Fig. 2 shows the detection results for the β-actin gene. The operating procedure for detection was the same simple procedure as that used for TMBs. The sensors were maintained at 25 °C for 10 min before the addition of target DNA,

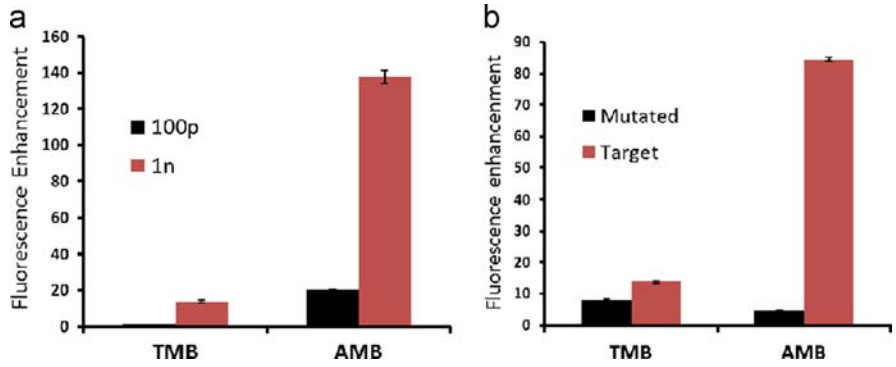

Fig. 1. Comparisons between AMB and TMB. (a) signal enhancements by TMB and AMB comparing with backgrounds in the absence of target DNA. Signal enhancements of AMB and TMB were recorded at the time of 30 min and 5 h after addition of the target sequence, respectively. Black bars and red bars indicated signal response of 100 pM and 1 nM DNA, respectively. (b) recognizing abilites of AMB and TMB towards single-base mismatch evaluated by signal enhancements comparing with backgrounds. The target DNA concentration is 1 nM. The black bars indicated the single-base mutated sequence and the red bars indicated the perfect matched sequence. All the concentrations of this kissed complex were 50 nM.

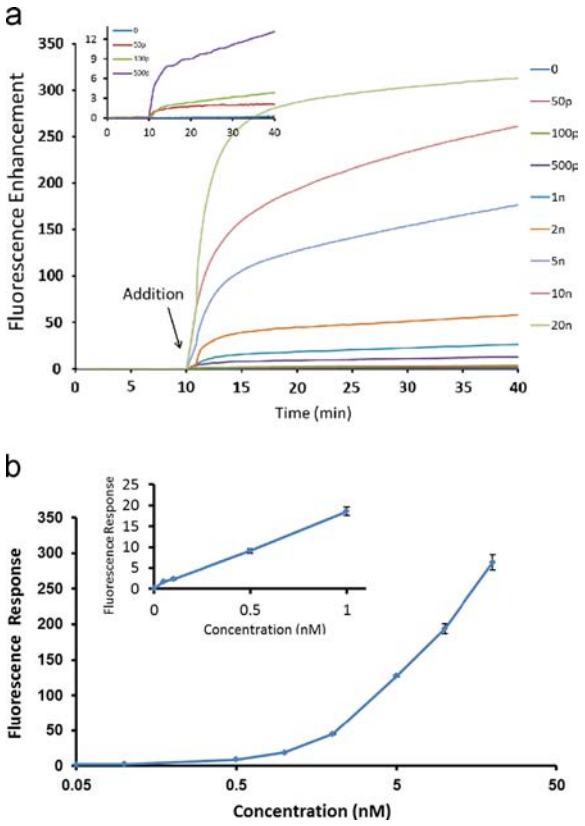

Fig. 2. Detection of a DNA sequence from the β-actin gene using external-opening kissing hairpins (see Scheme 1a for sketch). (a) monitoring fluorescence enhancements before and after addition of the target sequence. Concentrations of DNA were 0, 50 pM, 100 pM, 500 pM, 1 nM, 2 nM, 5 nM, 10 nM and 20 nM, respectively. The inset showed the enlarged curves for low concentrations. (b) signal response at the time of 10 min after addition of the target DNA. The inset showed the enlarged curves for low concentrations.

as indicated in Fig. 2a. In addition to the inherent superiority of AMBs, as described above, the detection process was accelerated greatly by introducing the external toehold. For example, the rate constant of this AMB with the external toehold when sensing 1 nM DNA was $1.25 \times 10^6\ M^{-1}\ min^{-1}$ (Fig. S3), which is much higher than that for the above asymmetric kissing hairpin. Fluorescence spectra of the detection samples after 10 min reaction were shown in Fig. S4. From 50 pM to 1 nM, the fluorescence enhancements were slight but detectable, when the concentration of target DNA was over 2 nM, greatly amplification of the signal could be observed. This rapid process only required ten minutes to provide sufficient enhancement to detect concentrations as low as 50 pM (Fig. 2b). The concentration range of the linear response is 0–5 nM (Fig. S5a). Naturally, a longer reaction time would lead to a stronger signal response. Thus, rational hairpin optimization could be used to construct AMBs for rapid gene detection.

Both TMBs and AMBs can detect specific proteins or small molecules through the integration of aptamer sequences that can recognize the target because both types of MB are based on the same mechanism of interaction. We chose the widely studied protein thrombin as our target for the aptamer sequence of the AMB. Fig. 3 presents the thrombin detection results. To facilitate protein binding, we placed one part of the aptamer sequence in the stem and another part outside. We also had to consider the fact that the binding of the hairpin DNA to the protein would make the rest of the hairpin stem unstable, leading it to open at room temperature. We thus rationally designed this hairpin, which had only 4 base pairs in the stem available after binding to thrombin, to enable activation (Table S1). Thrombin initially bound the aptamer sequence to open the recognition hairpin for amplification, and this binding behavior was clearly reflected in the CD spectra shown in Fig. 4. After addition of 2 μM thrombin into the solution, CD spectra were collected every six minutes during the followed 30-minute period at 25 °C. We could clearly observe the alterations near 280 nm which were the integrated signals combined by both the signal of G-quadruplex induced through thrombin and non-G-quadruplex part in the hairpin. CD signal of thrombin alone (the inset figure) did not influence the spectra near 280 nm. As it did for DNA detection, this AMB aptamer was also able to enhance the detected signal and lower the sensing limit for the protein. For example, the fluorescence signals were enhanced almost 14-fold over the background fluorescence level at 10 min after the addition of 100 nM thrombin (Fig. 3b), which is much greater than the enhancement obtained for the aptamer alone [38]. Thrombin could be detected at concentrations as low as 1 nM with a sufficient signal response (1.5-fold) after 10 min of amplification, the concentration range of the linear response is 0–200 nM (Fig. S5b). The introduction of other aptamer sequences could allow these AMBs to efficiently detect other proteins and small molecules.

It is well-known that the expression of specific miRNAs is closely associated with various cancers, and therefore miRNAs are very important markers for the early diagnosis of cancers [39]. To determine if AMBs could detect miRNA sensitively in vivo, we first investigated the use of this probe with different concentrations of synthetic miR-141. As shown in Fig. 5, the fluorescence emission peak remarkably increased with an increasing concentration of

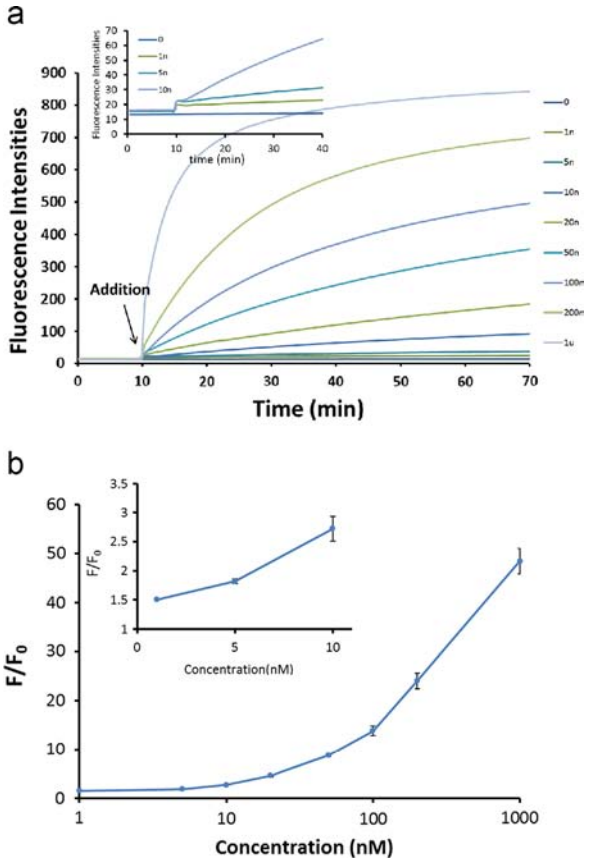

Fig. 3. Thrombin detection using rationally designed kissing hairpins (see Scheme 1b for sketch). (a) monitoring fluorescence intensities before and after addition of thrombin. Concentrations of thrombin were 0, 1 nM, 5 nM, 10 nM and 20 nM, 50 nM, 100 nM, 200 nM and 1 μM respectively. The inset showed the enlarged curves for low concentrations. (b) fluorescence response over background fluorescence with varying concentrations of thrombin at the time of 10 min after addition of the target DNA. *F* is the fluorescence intensity of each sample and F_0 is background fluorescence in the absence of any target. The inset showed the enlarged curves for low concentrations.

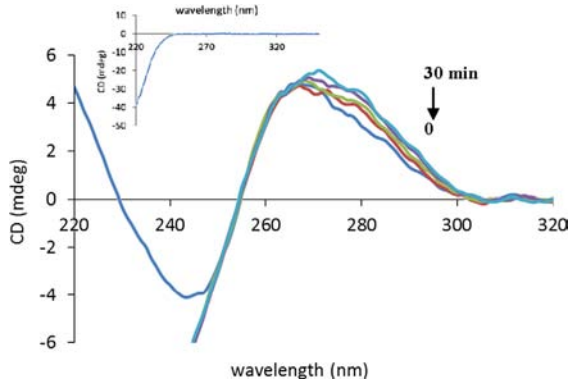

Fig. 4. CD observation of the interaction of thrombin with the aptamer-involved hairpin. The concentration of aptamer-involved hairpin was 2 μM.

miR-141 from 0 to 1 μM. The fluorescence intensity (F/F_0-1) at the concentration of 100 nM was equivalent to a 59-fold enhancement. This study indicated that miR-141 could be effectively and sensitively detected by the AMB.

We further evaluated the application of AMBs in living cells using laser confocal microscopy. MiR-141, as has been reported previously, is highly expressed in breast cancer cells and absent in cervical cancer cells [40,41]. We selected MDA-MB-231 cells to represent breast cancer and HeLa cells to represent cervical cancer.

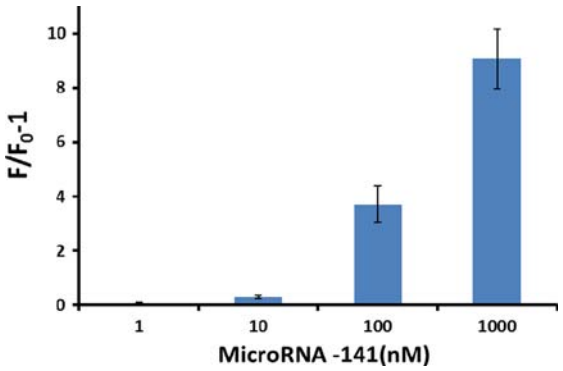

Fig. 5. Fluorescence emission spectra (excitation at 488 nm, emission at 530 nm) upon addition of miR-141. (F/F_0-1) as function of the concentrations of miR-141, where F_0 and F are the TET fluorescence signals in the absence and the presence of miR-141 (1 nM, 10 nM, 100nM, 1 μM), respectively.

Three different types of TET-labeled AMBs were positive control lacked the quencher (Table S1). These AMBs were transfected into both MDA-MB-231 and HeLa cells using liposomes. Laser confocal microscopy was performed at 4 h post infection (p.i.)(Fig. 6). The fluorescence of the positive control without the quencher was clearly observed, indicating that the transfection of the AMBs was effective (Fig. S6A,C). The negative control with the random recognition sequence yielded a very low fluorescence signal (Fig. S6B,D), indicating that the structure of the AMB was relatively stable, but the digestion of the AMB by cellular nucleases still contributed to a weak background signal. In contrast to the weak fluorescence signals for the MB probe in HeLa cells (Fig. 6B,D), an observable fluorescence signal was detected for the AMB (Fig. 6A,C). Given that the expression level of miR-141 in HeLa cells is low [41], this result demonstrates that the AMB probe could greatly enhance the detected signals and lower sensing limits for targets. The fluorescence signal for AMB detection in MDA-MB-231 cells (Fig. 6E,G) was higher than that in HeLa cells (Fig. 6A,C). And the fluorescence signal for TMB detection in MDA-MB-231 cells (Fig. 6F,H) is dispersive and weaker than that of AMB detection (Fig. 6E,G). These results indicate that MDA-MB-231 cells express a higher level of miR-141 (Fig. 6A,C), in agreement with previously results [40,41]. Therefore, the AMBs cannot only increase the detected signal and decrease the sensing limits for targets such as DNA, RNA, proteins and small molecules in vitro but also have a high sensitivity and a good amplification ability for in vivo detection.

4. Conclusions

In summary, we constructed autonomous DNA devices for hybridization amplification using molecular beacons. These AMBs greatly enhanced the detected signals and decreased the sensing limits, which made these MBs inherently superior. For nucleic acid detection, the AMBs also remarkably increased the ability to distinguish between the target sequence and a strand with a single base mutation, enabling the detection of single-nucleotide polymorphisms. AMBs can also detect proteins and small molecules when aptamer sequences are introduced into the AMBs. Although the limits of detection of AMBs are not as low as those of some reported enzymatic pathways [15–17], AMBs preserve the simplicity and flexibility of TMBs, which enzymatic methods lack. The simplicity of this approach is reflected in both the operating procedures and the design of the sensing element. Similar to TMBs, AMBs can detect targets by simple mixing, without any further steps, and their designs are simple and can be easily extended for various targets. This flexibility means that

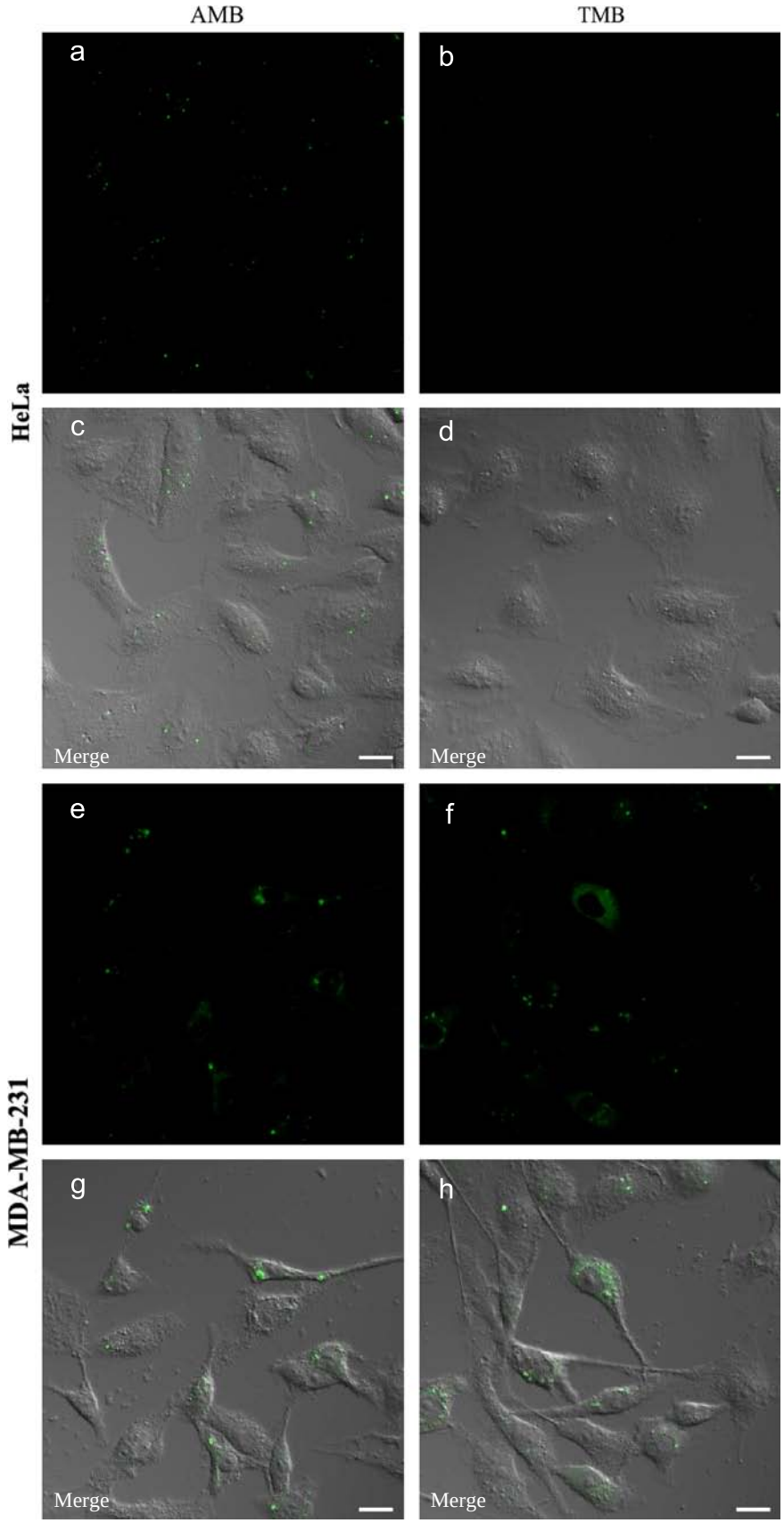

Fig. 6. Confocal laser scanning microscopy analysis of HeLa cells (A-D) and MDA-MB-231 cells (E-H) using a 40 × objective at 4 h p.i.. Images all using Ex 488, Em 515. A,C,E, G: cells detected by designed AMBs. B,D,F,H: cells detected by designed MBs. The white bar equals 20 μm.

these AMBs, such as TMBs, can be modified and can be linked to other components, such as nanoparticles, electrodes and other solid surfaces, to achieve various types of signal transduction. Additionally, AMBs can be used to detect miRNAs in living cells, especially when the expression level is low. The detection of miRNAs in single cells can be used to study the details of miRNAs and their association with diseases. Therefore, this technology will have a wide range of applications in bio-detection.

Acknowledgments

The authors thank the National Basic Research Program of China (973 Program)(2012CB720600, 2012CB720603), the National Science of Foundation of China (Nos. 91213302, 30973605, 21072115), the National Grand Program on Key Infectious Disease (2012ZX10003002-014), Open funding of the State Key Laboratory of Bioorganic, Program for Changjiang Scholars, Innovative Research Team in University (IRT1030)and Natural Products Chemistry, Shanghai Institute of Organic Chemistry, the Chinese Academy of Sciences.

Appendix A. Supplementary material

Supplementary data associated with this article can be found in the online version at http://dx.doi.org/10.1016/j.talanta.2013.11.038.

References

[1] S. Tyagi, F.R. Kramer, Nat. Biotechnol. 14 (1996) 303–308.
[2] K. Wang, Z. Tang, C. Yang, J.Y. Kim, X. Fang, W. Li, Y. Wu, C.D. Medley, Z. Cao, J. Li, P. Colon, H. Lin, W. Tan, Angew. Chem. Int. Ed. Engl. 48 (2009) 856–870.
[3] W. Tan, K. Wang, T.J. Drake, Curr. Opin. Chem. Biol. 8 (2004) 547–553.
[4] B. Dubertret, M. Calame, A.J. Libchaber, Nat. Biotechnol. 19 (2001) 365–370.
[5] J.F. Lovell, H. Jin, K.K. Ng, G. Zheng, Angew. Chem. Int. Ed. Engl. 49 (2010) 7917–7919.
[6] K.C. Jayagopal, Halfpenny, J.W. Perez, D.W. Wright, J. Am. Chem. Soc. 132 (2010) 9789–9796.
[7] H. Fan, K.W. Plaxco, A.J. Heeger, Proc. Natl. Acad. Sci. USA 100 (2003) 9134–9137.
[8] X. Zuo, Y. Xiao, K.W. Plaxco, J. Am. Chem. Soc. 13 (2009) 6944–6945.
[9] E. Farjami, L. Clima, K. Gothelf, E.E. Ferapontova, Anal. Chem. 83 (2011) 1594–1602.
[10] M. Culha, D.L. Stokes, G.D. Griffin, T. Vo-Dinh, J. Biomed. Opt. 9 (2004) 439–443.
[11] N. Venkatesan, Y.J. Seo, B.H. Kim, Chem. Soc. Rev. 37 (2008) 648–663.
[12] R. Fu, K. Jeon, C. Jung, H.G. Park, Chem. Commun. 47 (2011) 9876–9878.
[13] H. Lee, Y. Li, A.W. Wark, R.M. Corn, Anal. Chem. 77 (2005) 5096–5100.
[14] S. Sando, A. Narita, K. Abe, Y. Aoyama, J. Am. Chem. Soc. 127 (2005) 5300–5301.
[15] L.M. Lu, X.B Zhang, R.M Kong, B. Yang, W. Tan, J. Am. Chem. Soc. 133 (2011) 11686–11691.
[16] X. Zuo, F. Xia, Y. Xiao, K.W. Plaxco, J. Am. Chem. Soc. 132 (2010) 1816–1818.
[17] Y. Weizmann, M.K. Beissenhirtz, Z. Cheglakov, R. Nowarski, M. Kotler, I. Willner, Angew. Chem. Int. Ed. 45 (2006) 7384–7388.
[18] S. Nakayama, H.O. Sintim, J. Am. Chem. Soc. 131 (2009) 10320–10333.
[19] M. Deng, D. Zhang, Y. Zhou, X. Zhou, J. Am. Chem. Soc. 130 (2008) 13095–13102.
[20] B.J. Lam, G.F. Joyce, Nat. Biotechnol. 27 (2009) 288–292.
[21] F. Wang, J. Elbaz, R. Orbach, N. Magen, I. Willner, J. Am. Chem. Soc. 133 (2011) 17149–17151.
[22] Y. Song, L. Cui, J. Wu, W. Zhang, W.Y. Zhang, H. Kang, C.J. Yang, Chem. Eur. J 17 (2011) 9042–9046.
[23] W. Zhao, M.M. Ali, M.A. Brook, Y. Li, Angew. Chem. Int. Ed. 47 (2008) 6330–6337.
[24] J. Chen, J. Zhang, Y. Guo, J. Li, F. Fu, H. Yang, G. Chen, Chem. Commun. 47 (2011) 8004–8006.
[25] J. Bath, A.J. Turberfield, Nat. Nanotechnol. 2 (2007) 275–284.
[26] Y. Krishnan, F.C. Simmel, Angew. Chem. Int. Ed. 50 (2011) 3124–3156.
[27] L. Qian, E. Winfree, J. Bruck, Nature 475 (2011) 368–372.
[28] D.Y. Zhang, A.J. Turberfield, B. Yurke, E. Winfree, Science 318 (2007) 1121–1125.
[29] G. Seelig, D. Soloveichik, D.Y. Zhang, E Winfree, Science 314 (2006) 1585–1588.
[30] P. Yin, H.M. Choi, C.R. Calvert, N.A. Pierce, Nature 451 (2008) 318–322.
[31] R.M. Dirks, N.A. Pierce, Proc. Natl. Acad. Sci. USA 101 (2004) 15275–15278.
[32] H.M. Choi, J.Y. Chang, A. Trinh, J.E. Padilla, S.E. Fraser, N.A. Pierce, Nat. Biotechnol. 28 (2010) 1208–1212.
[33] S.J. Green, D. Lubrich, A.J. Turberfield, Biophys. J. 91 (2006) 2966–2975.
[34] J.S. Bois, S. Venkataraman, H.M. Choi, A.J. Spakowitz, Z.G. Wang, N.A. Pierce, Nucleic Acids Res. 33 (2005) 4090–4095.
[35] J. Turberfield, J.C. Mitchell, B. Yurke, A.P. Mills, M.I. Blakey, F.C. Simmel, Phys. Rev. Lett. 90 (2003) 118102.
[36] A.D. Li, X. Ellington, Chen, Nucleic Acids Res. 39 (2011) e110.
[37] Y. Zhang, E. Winfree, J. Am. Chem. Soc. 131 (2009) 17303–17314.
[38] R. Nutiu, Y. Li, J. Am. Chem. Soc. 125 (2003) 4771–4778.
[39] J. Lu, G Getz, E.A. Miska, E. Alvarez-Saavedra, J. Lamb, D. Peck, A. Sweet-Cordero, B.L. Ebert, R.H. Mak, A.A. Ferrando, J. Downing, R.T. Jacks, H.R. Horvitz, T.R. Golub, Nature 435 (2005) 834–838.
[40] B.C. Yin, Y.Q. Liu, B.C. Ye, J. Am. Chem. Soc. 134 (2012) 5064–5067.
[41] P. Landgraf, M. Rusu, R. Sheridan, A. Sewer, N. Iovino, A. Aravin, S. Pfeffer, A. Rice, A.O. Kamphorst, M. Landthaler, C. Lin, N.D. Socci, L. Hermida, V. Fulci, S. Chiaretti, R. Foà, J. Schliwka, U. Fuchs, A. Novosel, R.U. Müller, B. Schermer, U. Bissels, J. Inman, Q. Phan, M. Chien, D.B. Weir, R. Choksi, G. De Vita, D. Frezzetti, H.I. Trompeter, V. Hornung, G. Teng, G. Hartmann, M. Palkovits, R. Di Lauro, P. Wernet, G. Macino, C.E. Rogler, JW. Nagle, J. Ju, F.N. Papavasiliou, T. Benzing, P. Lichter, W. Tam, M.J. Brownstein, A. Bosio, A. Borkhardt, J.J. Russo, C. Sander, M. Zavolan, T. Tuschl, Cell 129 (2007) 1401–1414.